Dalton Transactions

PAPER

Ga[NO2A-*N*-(α-amino)propionate] chelates: synthesis and evaluation as potential tracers for ^{68}Ga PET†

Cite this: *Dalton Trans.*, 2014, **43**, 8037

Miguel F. Ferreira,[a] Goretti Pereira,[a] João P. André,[a] M. I. M. Prata,[b] Paula M. T. Ferreira,[a] José A. Martins*[a] and Carlos F. G. C. Geraldes[c,d]

Received 6th February 2014,
Accepted 7th March 2014

DOI: 10.1039/c4dt00386a

www.rsc.org/dalton

The availability of commercial ^{68}Ge/^{68}Ga cyclotron-independent $^{68}Ga^{3+}$ generators is making Positron Emission Tomography (PET) accessible to most hospitals, which is generating a surge of interest in the design and synthesis of bi-functional chelators for Ga^{3+}. In this work we introduce the NO2A-*N*-(α-amino)propionic acid family of chelators based on the triazacyclononane scaffold. Complexation of the parent NO2A-*N*-(α-amino)propionic acid chelator and of a low molecular weight (model) amide conjugate with Ga^{3+} was studied by ^{1}H and ^{71}Ga NMR. The Ga^{3+} chelate of the amide conjugate shows pH-independent N_3O_3 coordination in the pH range 3–10 involving the carboxylate group of the pendant propionate arm in a 6 member chelate. For the Ga[NO2A-*N*-(α-amino)propionate] chelate, a reversible pH-triggered switch from Ga^{3+} coordination to the carboxylate group to coordination to the amine group of the propionate arm was observed upon pH increase/decrease in the pH range 4–6. This phenomenon can conceivably constitute the basis of a physiological pH sensor. Both complexes are stable in the physiological range. The [^{67}Ga][NO2A-*N*-(α-benzoylamido)propionate] chelate was found to be stable in human serum. Biodistribution studies of the $^{67}Ga^{3+}$-labeled pyrene butyric acid conjugate NO2A-*N*-(α-pyrenebutanamido)propionic acid revealed that, despite its high lipophilicity and concentration-dependent aggregation properties, the chelate follows mainly renal elimination with very low liver/spleen accumulation and no activity deposition in bones after 24 hours. Facile synthesis of amide conjugates of the NO2A-*N*-(α-amino)propionic acid chelator, serum stability of the Ga^{3+} chelates and fast renal elimination warrant further evaluation of this novel class of chelators for PET applications.

Introduction

Endowing thermodynamically stable and kinetically inert metal chelates with conjugability is the subject of intensive research given the plethora of properties offered by metal ions for imaging and therapy. Non-functionalised metal chelates exhibit high hydrophilicity, distribution into the interstitial compartment, fast renal clearance and featureless biodistribution profiles. Delivering metal chelates to injury sites, for imaging and/or therapeutic purposes, allows reducing the dose and background signals and minimizes potential harmful side effects on non-target organs – especially critical with complexes of metal-radioisotopes.

Positron Emission Tomography (PET) is well established in clinical diagnosis for functional imaging thanks to its remarkably high detection sensitivity, relatively high spatial resolution and potential to quantify tracer uptake within lesions. ^{18}F, ^{11}C, ^{13}N are the most widely used radionuclides for PET imaging due to their positron emission properties and short lifetimes. These radionuclides are covalently incorporated into biomolecules (sugars, amino acids, *etc.*) through chemical synthesis, starting from simple precursor molecules/ions generated in dedicated cyclotron units.[1] Molecules labeled with ^{11}C and ^{13}N are indistinguishable from the natural abundance stable isotope unlabelled molecules undergoing the same metabolic pathways. C-2 ^{18}F labeled glucose (2-deoxy-2-[^{18}F]fluoroglucose – FDG) is the most widely used tracer in

[a]*Centro de Química (CQ-UM), Universidade do Minho, Campus de Gualtar, 4710-057 Braga, Portugal. E-mail: jmartins@quimica.uminho.pt*
[b]*ICNAS and IBILI, Faculty of Medicine, University of Coimbra, 3000-548 Coimbra, Portugal*
[c]*Department of Life Sciences, Faculty of Science and Technology, University of Coimbra, P.O. Box 3046, 3001-401 Coimbra, Portugal*
[d]*Chemistry Centre, University of Coimbra, Rua Larga, 3004-535 Coimbra, Portugal*

†Electronic supplementary information (ESI) available: 1D proton and 2D COSY NMR spectrum (600 MHz) of GaL_1 at pH 3.0 (Fig. S1); 1D proton and 2D COSY NMR spectrum (600 MHz) of GaL_1 at pH 4.0 (Fig. S2); UV-Vis spectra for the free ligand L_3 and the GaL_3 complex (1.0×10^{-5} M) (Fig. S3); Fluorescence spectra for L_3 in non-deoxygenated water over the concentration range 1.0×10^{-7} and 5×10^{-3} mol dm^{-3} (λ_{exc} = 345 nm) (Fig. S4); Optimized structure of GaL_3 (Mopac PM6 COSMO water implicit solvent) (Fig. S5). Computed log *P* for the GaL_2 and GaL_3 complexes after structure optimization with Mopac PM6 COSMO water implicit solvent (Table S1); Biodistribution, stated as percentage of injected dose per gram of organ (%ID g^{-1}), of $^{67}GaL_3$ in Wistar rats at 1 and 24 hours after i.v. injection (Table S2). See DOI: 10.1039/c4dt00386a

clinical PET imaging. Following uptake by the glucose transporters and phosphorylation, FDG is trapped inside cells as FDG-6-P, allowing visualization *in vivo* of glucose avid cells and tissues. ^{18}F decay allows the resulting 2-[^{18}OH]glucose to follow the normal glycolytic pathway.[2,3] ^{18}F, and especially ^{11}C and ^{13}N-labelled PET tracers, with half-lives of 109.8, 20.3, and 9.96 minutes, respectively, need to be produced *in loco* in dedicated cyclotron units, using fast, high yielding synthetic procedures coupled to expeditious purification schemes (operated remotely) to avoid substantial loss of activity.[1–3]

Many metal ion radionuclides (*e.g.* $^{68}Ga^{3+}$ and $^{64}Cu^{2+}$) also display positron emission properties suitable for PET imaging.[4] Amongst these, $^{68}Ga^{3+}$, with 89% positron branching accompanied by low photon emission (1077 keV, 3.22%) and a half life of 67.6 minutes, is suitable for labelling molecules with fast blood clearance.[5,6] The commercial availability of $^{68}Ge/^{68}Ga$ cyclotron-independent $^{68}Ga^{3+}$ generators is making PET imaging available to most hospitals.[7] Labeling (bio)molecules with metal ion radionuclides requires efficient pathways to attach covalently bi-functional chelators (post-conjugation labeling), or functionalized chelates (pre-conjugation labeling) to biomolecules.[4–7] High thermodynamic stability and kinetic inertness of the metal complexes are absolutely mandatory for safe and efficient PET imaging.[8–10] Transferrin, the iron transport protein, is the main competitor for Ga^{3+} in serum given the similar ionic radius and coordination properties of Fe^{3+} and Ga^{3+}.[11] In addition to stability, fast complexation, ideally at room temperature, and efficient purification procedures of labeled conjugates have to be taken into account in the design of new chelators for Ga^{3+} for use as PET tracers.[12] Moreover, complex formation with Ga^{3+}, obtained as $^{68}GaCl_3$ by elution of $^{68}Ge/^{68}Ga$ generators with diluted hydrochloric acid, must be carried out at pH values below 4 (usually in acetate or HEPES buffer) to avoid precipitation of Ga^{3+} as $Ga(OH)_3$.[13,14]

The coordination chemistry of Ga^{3+} is dominated by its hard character, preferring hard, charged base donors such as carboxylates, phosphonates and phosphinates in an octahedral geometry,[10] although it has also been shown to have good affinity for thiolates, such as TACN-TM (TACN-TM = 1,4,7-triazacyclononane-*N*,*N*′,*N*″-tris(mercaptoethyl)).[10,15] Poly(aminocarboxylates) and poly(aminophosphonates/phosphinates) are the most efficacious chelators for Ga^{3+}. Macrocyclic, DOTA-type (DOTA = 1,4,7,10-tetrazacyclododecane-1,4,7,10-tetraacetic acid) and NOTA-type (NOTA = 1,4,7-triazacyclononane-1,4,7-triacetic acid) chelators form Ga^{3+} complexes displaying exceptional thermodynamic stability and kinetic inertness.[12,16–18] Ga^{3+} complexes of linear, DTPA[19] (DTPA = diethylenetriamine pentaacetic acid) and EDTA-type[20] (EDTA = ethylenediaminetetraacetic acid) chelators were found to be kinetically too unstable for *in vivo* use, despite the high thermodynamic stability of its $Ga(EDTA)^-$ and $Ga(DTPA)^{2-}$ complexes.[21,22] DOTA-monoamide (octadentate) chelators, developed originally as Gd^{3+} complexing agents for use as Contrast Agents (CA) for Magnetic Resonance Imaging (MRI), despite forming Ga^{3+} complexes exhibiting lower thermodynamic stability and higher kinetic lability than the parent $Ga(DOTA)^-$ complex, are still kinetically inert enough for *in vivo* PET.[12] The peptide conjugate [^{68}Ga](DOTATOC) (DOTATOC = DOTA, Tyr^3-octreotide) is used worldwide in hospitals for diagnosis of neuroendocrine tumors expressing somatostatin receptors.[23,24]

The macrocycle cavity of DOTA-type chelators, optimal for Ln^{3+} ions, is too big for Ga^{3+} complexation, thus originating distorted octahedral (N_4O_2) complexes.[10,12,23,24] Good matching of the macrocycle cavity of NOTA with the ionic radius of Ga^{3+} results in Ga(NOTA) complexes exhibiting exceptional thermodynamic stability and kinetic inertness.[16,17] Moreover, NOTA-type chelators display faster Ga^{3+} chelation kinetics at lower temperatures than DOTA-type chelators.[25] NOTA-monoamide conjugates, although amenable through *facile* synthetic routes, are likely to result in complexes exhibiting lower thermodynamic stability and higher kinetic lability than their parent Ga(NOTA) complex, compromising their potential for biological applications.[26] Replacing an acetate arm on the NOTA scaffold, by an acetate group α-substituted with a reactive group, endows the NOTA scaffold with conjugability whilst preserving its N_3O_3 denticity mandatory for stable coordination with Ga^{3+}. The aspartate and glutamate derivatives of NOTA, NODASA (NODASA = 1,4,7-triazacyclononane-*N*-succinic-*N*′,*N*″-diacetic acid)[27] and NODAGA (NODAGA = 1,4,7-triazacyclononane-*N*-glutaric-*N*′,*N*″-diacetic acid),[28] respectively, are the gold standards for the synthesis of targeted Ga^{3+} tracers for PET. More recently, the TRAP (TRAP = 1,4,7-triazacyclononane-1,4,7-tris(methylenephosphinic acid)) family of chelators, generated by replacement of the pendant carboxylates by phosphinate groups on the triazacyclononane macrocycle scaffold, revealed excellent chelating properties for Ga^{3+} allied to conjugability.[29–31] Tris-NODASA/NODAGA[32] and tris-TRAP[29] derivatives allow *facile* preparation of multivalent conjugates with biomolecules such as peptides, exhibiting enhanced avidity (affinity and/or specificity) for cellular receptors. Pendant reactive groups on the ethylenediamine bridges of the NOTA scaffold allow also bioconjugation whilst retaining the high thermodynamic stability and kinetic inertness of the Ga(NOTA) complex, although at the expense of difficult and lengthy synthetic pathways.[33]

In our efforts to obtain thermodynamically stable and kinetically inert conjugates of metal chelates as potential medical imaging agents, we have reported recently efficient methodologies for the synthesis of the DO3A-*N*-(α-amino)propionate chelator[34] and for the preparation of amide conjugates.[35–37] The Gd[DO3A-*N*-(α-amino)propionate] chelate and its amide conjugates combine high thermodynamic stability and kinetic inertness with (fast) water exchange properties, ideal for attaining high relaxivities at (intermediate/high) fields relevant for magnetic resonance imaging.[34–37] In this work we extend the synthetic methodologies developed for DO3A-*N*-(α-amino)propionate chelators to the triazacyclononane scaffold. This includes the NO2A-*N*-(α-amino)propionic acid ($\mathbf{L_1}$) chelator and the two amide derivatives NO2A-*N*-(α-benzoylamido)-propionic acid ($\mathbf{L_2}$) and NO2A-*N*-(α-pyrenebutanamido)propionic acid ($\mathbf{L_3}$) (see Scheme 1). The complexation of the new chela-

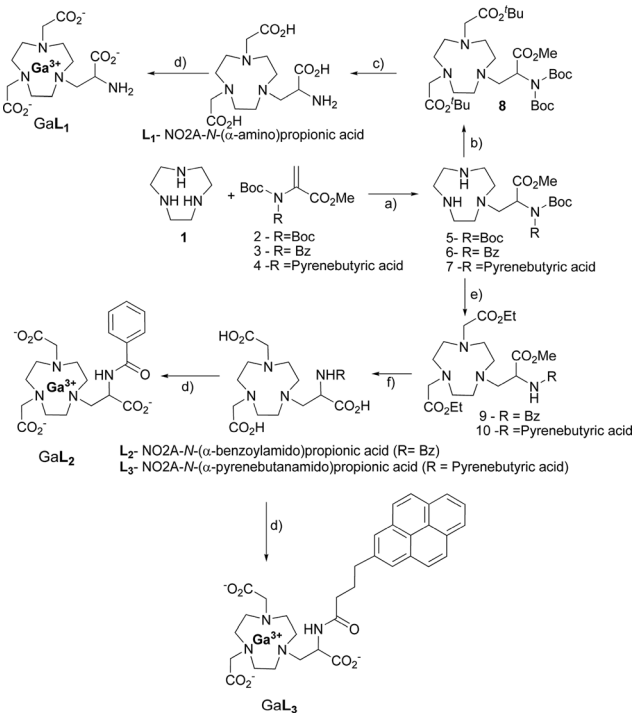

Scheme 1 Synthetic pathway for the metal chelators NO_2A-*N*-(α-amino)propionic acid ($\mathbf{L_1}$), NO_2A-*N*-(α-benzoylamido)propionic acid ($\mathbf{L_2}$) and NO_2A-*N*-(α-pyrenebutanamido)propionic acid ($\mathbf{L_3}$). (a) K_2CO_3/MeCN; (b) *tert*-butyl bromoacetate, K_2CO_3/MeCN; (c) i. hydrochloric acid/EtOH, ii. Dowex-1X2-OH^-, elution with diluted hydrochloric acid; (d) $GaCl_3{\cdot}xH_2O$; (e) i. TFA/CH_2Cl_2; ii. ethyl bromoacetate, K_2CO_3/MeCN; (f) Dowex-1X2-OH^-, elution with diluted hydrochloric acid.

tors with Ga^{3+} was studied by multinuclear NMR (^1H, ^{71}Ga). The luminescence properties of the Ga$\mathbf{L_3}$ complex were also analysed in order to evaluate its potential as a bimodal PET/optical imaging agent. Serum stability and biodistribution studies were also performed to evaluate the potential of the new chelators as $^{68}Ga^{3+}$-labeled PET tracers.

Results and discussion

Synthesis and characterization

In this work we aimed at extending the synthetic methodologies developed for DO3A-*N*-(α-amino)propionate chelators[34–37] to the triazacyclononane scaffold, to explore the coordination properties of NO2A-*N*-(α-amino)propionic acid chelators for Ga^{3+} as potential tracers for PET imaging (Scheme 1).

Michael addition of the Boc_2-Δ-AlaOMe (**2**)[34] and Boc-(amide)-Δ-AlaOMe blocks **3**[36] and **4**[37] to triazacyclononane (**1**) proceeds smoothly in acetonitrile at room temperature, using K_2CO_3 as a base, in 3–4 hours, as reported before for the *cyclen* analogue. An excess of triazacyclononane, 1.5 molar equivalents, affords the monoalkylated nonanes as the main reaction products. Small amounts of bis- and tris-alkylated derivatives are easily removed by flash chromatography. Further *N*-alkylation of nonane **5** with *tert*-butyl bromoacetate, followed by sequential deprotection with hydrochloric acid (4 M) and Dowex-1X2-OH^- resin, and elution with diluted hydrochloric acid afforded the NO2A-*N*-(α-amino)propionic acid chelator ($\mathbf{L_1}$) as hydrochloride in (non-optimised) 36% overall yield. Alkylation of monoalkylated cyclen **5** with ethyl bromoacetate offers the opportunity to deprotect selectively the amine group for further conjugation.[35] This (*direct*) conjugation pathway was not pursued in this work. Instead, we have explored the *indirect pathway* for preparing amide conjugates of the NO2A-*N*-(α-amido)propionic acid chelator.[36] The NO2A-*N*-(α-benzoylamido)propionic acid chelator ($\mathbf{L_2}$) is likely to result in soluble non-associating chelates; the pyrenyl conjugate NO2A-*N*-(α-pyrenebutanamido)propionic acid chelator ($\mathbf{L_3}$) was designed as a self-assembling, fluorescent chelator, potentially useful for bimodal PET/fluorescence imaging.[37] Michael addition of Boc-(dehydroamide)-Δ-AlaOMe blocks **3** and **4** introduces directly the amide (targeting/kinetic modulator) group into the triaza scaffold. Removing the Boc group at the monoalkylated stage averts retro-elimination during the second alkylation step. One step deprotection of the ester protected prochelators **9** and **10** with Dowex-1X2-OH^- resin affords the fully deprotected chelators $\mathbf{L_2}$ and $\mathbf{L_3}$ as hydrochlorides, after elution with aqueous hydrochloric acid.

Many other amide conjugates are accessible using the expeditious methodologies described in this work.

^1H and ^{71}Ga NMR studies

Given the current interest in ^{68}Ga PET, unleashed by the commercial availability of cyclotron-independent ^{68}Ga generators,[4–7] we carried out a multinuclear NMR study (^1H and ^{71}Ga) of the Ga$\mathbf{L_1}$ and Ga$\mathbf{L_2}$ chelates to ascertain the coordination properties of the novel chelators and their potential for PET imaging applications.

^{71}Ga (38.89%) is a quadrupolar nucleus (I = 3/2) exhibiting a relatively high receptivity and a wide range of chemical shifts.[38] The quadrupolar nature of its relaxation mechanism leads to NMR signals whose linewidth is sensitive to the symmetry of the coordination environment. Spherical, octahedral, cubic and tetrahedral symmetries should, in principle, originate sharp ^{71}Ga NMR signals. This is the case for NOTA-type triazamacrocyclic complexes, whose predominant coordination geometry is distorted octahedral, as opposed to DOTA-type tetraazamacrocyclic complexes like Ga(DOTA)- and its monoamide derivatives, whose low coordination symmetry makes their ^{71}Ga NMR signals too broad to be detected.[12] The chemical shift is characteristic of the coordination geometry of the metal ion.[39,40]

The pH dependence of the ^1H (Fig. 3) and ^{71}Ga NMR spectra (Fig. 1) for the Ga$\mathbf{L_1}$ and Ga$\mathbf{L_2}$ complexes was studied in D_2O to probe the coordination environment of the Ga^{3+} metal ion.

Table 1 summarizes the ^{71}Ga NMR chemical shifts and linewidths for the species observed in solution for the Ga$\mathbf{L_1}$ and Ga$\mathbf{L_2}$ complexes studied in this work, compared with other triazamacrocyclic complexes reported in the literature (Fig. 2).

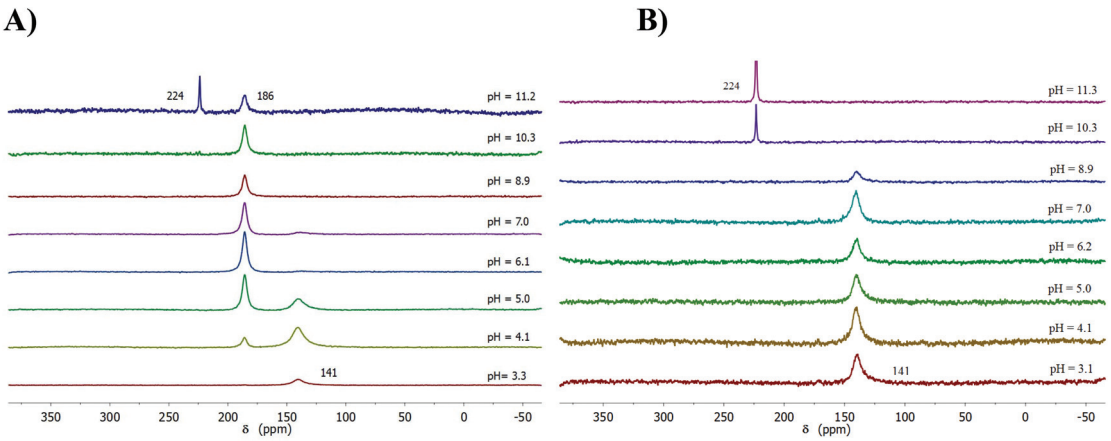

Fig. 1 pH dependence of the ^{71}Ga NMR spectra for: (A) the Ga**L**$_1$ and (B) Ga**L**$_2$ complexes (400 MHz, 20 mM in D_2O, 25 °C).

Table 1 ^{71}Ga NMR chemical shifts and linewidths for the Ga**L**$_1$ and Ga**L**$_2$ complexes studied in this work, compared with other triazamacrocyclic complexes reported in the literature[40]

Complex	δ (ppm)	$\Delta\nu_{1/2}$ (Hz)	Coordination
Ga**L**$_1$ [a]	+141	900	N_3O_3
	+186	550	N_4O_2
Ga**L**$_2$ [a]	+140	900	N_3O_3
Ga(**NOTA**)[b]	+171	235	N_3O_3
Ga(**NO2A-*N*-methylacetamide**)[c]	+171	283	N_3O_3
Ga(**NO2A-*N*-benzylacetamide**)[c]	+175	9085	N_4O_2
	+170	279	N_3O_3
	+174	4818	N_4O_2
Ga(**NOTP**)[d]	+110	434	N_3O_3
Ga(**NOTMP**)[e]	+136	215	N_3O_3
Ga(**TRAP-H**)[f]	+132	154	N_3O_3
	+134	200	N_3O_3
	+138	186	N_3O_3
	+141	162	N_3O_3

[a] This work. [b] Ref. 17,41. [c] Ref. 42. [d] Ref. 43. [e] Ref. 44. [f] Ref. 30.

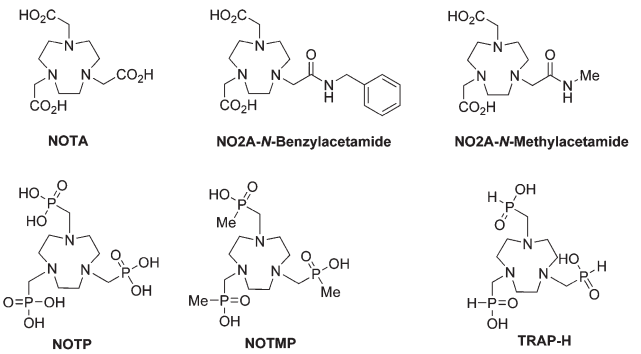

Fig. 2 Structure of triazacyclononane ligands compared in Table 1 and discussed in the manuscript: NOTP (1,4,7-triazacyclononane-*N*,*N*′,*N*″-tris(methylenephosphonic) acid); NOTMP (1,4,7-triazacyclononane-*N*,*N*′,*N*″-tris(methylene(methylphosphinate))); TRAP-H (1,4,7-triazacyclononane-1,4,7-tris(methylenephosphinic) acid).

The number and population of the species present over the pH range 3–11, as well as their chemical shifts and linewidths, are quite different for the Ga**L**$_1$ and Ga**L**$_2$ complexes.

The Ga**L**$_2$ complex displays only one ^{71}Ga NMR signal in the pH range 3–9: a singlet at δ = 140 ppm with a relatively large linewidth, $\Delta\nu_{1/2}$ = 900 Hz. Above pH 9.0, hydroxide catalyzed demetallation leads to the formation of the $[Ga(OH)_4]^-$ species characterized by a sharp signal at δ = 224 ppm.[40] In contrast, the ^{71}Ga NMR spectrum of the Ga**L**$_1$ chelate is pH dependent. At pH 3.0 there is only one signal with a chemical shift (141 ppm) and width (900 Hz) identical to that displayed by the Ga**L**$_2$ complex. A new sharper ($\Delta\nu_{1/2}$ = 550 Hz) signal at δ = 186 ppm becomes apparent at pH 4.1. The intensity of this signal increases, at the expense of the signal at δ = 141 ppm, when the pH increases, eventually becoming the only signal in the pH range 6–10. At pH 11, the $[Ga(OH)_4]^-$ species is also present. This process is fully reversible, reproducing the same features upon pH decrease. These results strongly suggest that for the amide complex Ga**L**$_2$, the coordination polyhedron is likely to be represented by a distorted octahedron involving the carboxylate group of the propionate arm to form a six member chelate (coordination polyhedron N_3O_3). Although coordination through the amide nitrogen, forming a five member chelate, is also possible, the preference of the hard Ga^{3+} ion for the carboxylate group is likely to compensate for the energy cost of forming a six member chelate.[42] The Ga**L**$_1$ chelate seems to undergo the same chelation scheme (N_3O_3) as the amide complex at low pH, presumably due to the unavailability of the protonated amine group for binding. At higher pH (6–11) the formation of a five member chelate with the deprotonated amine group (coordination polyhedron N_4O_2) seems to be more favorable than the formation of a six member chelate with the harder carboxylate group. The N_4O_2 chelation mode for the Ga**L**$_1$ chelate (all five member chelates) is likely to generate a coordination polyhedron of higher symmetry, similar to Ga(NOTA), than the N_3O_3 geometry involving a six member chelate – thus, the sharper ^{71}Ga NMR signal and

higher chemical shift of the N_4O_2 isomer of Ga**L**$_1$ at pH 6–11. For the Ga**L**$_3$ complex at 20 mM concentration, the ^{71}Ga NMR spectrum becomes too broad to be measured, reflecting provably the micellar state of the complex.[45] Both Ga**L**$_1$ and Ga**L**$_2$ complexes are stable in the physiological pH range undergoing hydroxide catalyzed demetallation above pH 10 and 9, respectively. This is apparent in the ^{71}Ga NMR spectra by the disappearance of the signals assigned to the complexes and by the appearance of the sharp signal at δ = 224 ppm, assigned to the $[Ga(OH)_4]^-$ ion. All known Ga^{3+} complexes undergo hydroxide catalyzed demetallation in the alkaline pH region.[40] In this respect, the Ga**L**$_1$ complex seems to be more stable than the amide conjugate Ga**L**$_2$ chelate, requiring a higher pH for complete demetallation. This can be ascribed to the preference for N_4O_2 coordination of the Ga**L**$_1$ complex at high pH, compared to the N_3O_3 coordination of Ga**L**$_2$. A similar isomerization process involving coordination of the Ga^{3+} ion to the nitrogen or oxygen atom of the amide linkage (five member chelates) has been observed for the Ga(**NO2A-*N*-benzylacetamide**) and Ga(**NO2A-*N*-methylacetamide**) complexes (Fig. 2 and Table 1), both in the solid state and in aqueous solution. At low pH the N_3O_3 coordination predominates over N_4O_2 coordination.[42] As can be seen in Table 1, the two isomers of the Ga(**NO2A-*N*-benzylacetamide**) and Ga(**NO2A-*N*-methylacetamide**), involving in both cases five member chelates, show much smaller shift differences and are much broader than the isomers found in the present study for Ga**L**$_1$. The phosphonate complex Ga(NOTP)[43] and some phosphinate complexes, like Ga(NOTMP),[44] lead to the presence of only one species in solution. In all the NOTA-type complexes with N_3O_3 coordination, the Ga^{3+} ion is placed between twisted trigonal O_3 and N_3 planes, an arrangement which leads to chiral complexes. This is caused by the combination of the conformation of the chelate rings in the macrocyclic moiety ($\delta\delta\delta/\lambda\lambda\lambda$) with the helicity of the coordinated pendant arms (Δ/Λ), which leads to two diastereoisomeric pairs $\Delta\delta\delta\delta/\Lambda\lambda\lambda\lambda$ and $\Lambda\delta\delta\delta/\Delta\lambda\lambda\lambda$. In the NOTA derivatives bearing three phosphinate pendant arms, those chiralities are combined with the *R*/*S* chirality of the phosphorus atom upon metal coordination, leading to four possible diastereomeric pairs, *Λδδδ –RRR*/*Δλλλ–SSS*, *Λδδδ–RRS*/*Δλλλ–SSR*, *Λδδδ–RSS*/*Δλλλ–SRR* and *Λδδδ–SSS*/*Δλλλ–RRR*. In the Ga^{3+} phosphinate complexes with alkyl substituents (CH_3 in Ga(NOTMP)[44] or CH_2OH in Ga(TRAP-OH),[30] only the *Λδδδ–RRR*/*Δλλλ–SSS* diastereoisomer is observed in solution, leading to a single ^{71}Ga signal, while for more electron-withdrawing substituents, like H in Ga(TRAP-H),[30] the full mixture of possible isomers is observed in solution as a set of four narrow resonances with very small shift differences (Table 1).

The 1D ^{1}H and 2D COSY and NOESY spectra of the Ga**L**$_1$ complex solutions were also obtained at 25 °C in the pH range 3.0–9.0, and at pH 3.0–5.5 for Ga**L**$_2$. The proton resonance signals from the macrocyclic backbones were only tentatively assigned due to superimposed multiplet signals in the 3.7–2.8 ppm range (Fig. S1 and S2†). The NCH_2CO_2H acetate arm protons give a multiplet at 3.85 ppm, while the phenyl group of Ga**L**$_2$ originates three multiplets at 7.70, 7.45 and 7.40 ppm with a 2 : 2 : 1 intensity ratio, corresponding to the *ortho*, *para* and *meta* CH protons. The most informative resonances correspond to the NCH_2CH protons of the substituted propionate arm of the complexes, in the form of a characteristic ABX pattern, with the CH proton resonances outside the envelope of other protons (Fig. S1 and S2†). The AB patterns of the CH_2 signal coupled to the CH group (NCH_2CH) could be traced to the COSY spectra of both complexes (Fig. S1 and S2†). In the case of Ga**L**$_2$ the CH multiplet has a single component at 5.05 ppm (Fig. 3), in accordance with the single ^{71}Ga resonance at +140 ppm, corresponding to N_3O_3 coordination (Fig. 1). In the case of Ga**L**$_1$ the CH proton signals are pH-dependent, in parallel with what was observed for the ^{71}Ga NMR spectra (Fig. 3). Whereas at pH 3.3, it consists of a single multiplet (doublet of triplets) at 4.47 ppm (labeled I), corresponding to the single ^{71}Ga resonance at 141 ppm (N_3O_3 coordination isomer), at pH 4.1 there are two CH multiplets at 4.50 (I) and 4.38 ppm (II), corresponding to the ^{71}Ga signals at 141 and 186 ppm, assigned to the N_3O_3 and N_4O_2 isomers, respectively. The relative intensity of the N_4O_2 signals (4.38 ppm and 186 ppm) increases with pH in relation to the N_3O_3 signals (4.50 and 141 ppm) and at pH 6.1 only the 4.38 ppm signal is present. The corresponding CH_2 multiplets are observed between 3.60 and 3.20 ppm (Fig. S1 and S2†). Therefore, the proton NMR spectra confirm the isomer information provided by the ^{71}Ga NMR spectra.

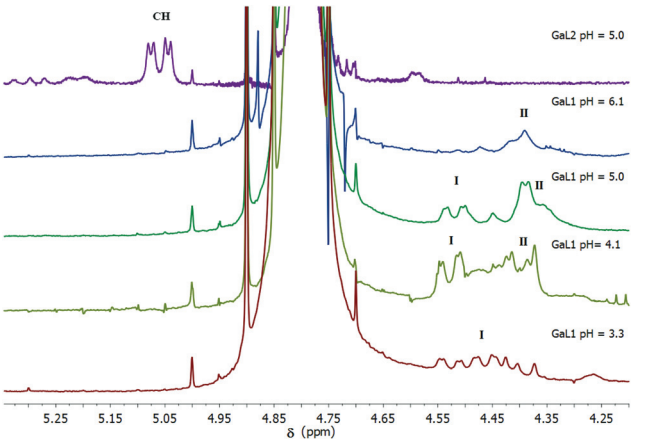

Fig. 3 pH dependence of the proton NMR resonances of the CH protons of the propionate side arm of the Ga**L**$_1$ and Ga**L**$_2$ complexes (400 MHz, 20 mM in D_2O, 25 °C).

Fluorescence studies

The Ga**L**$_3$ complex was designed to have properties compatible with a bimodal PET/fluorescence imaging agent. The lipophilic pyrene moiety was selected due to its special aggregation-sensitive fluorescence properties.[37,46] The absorption (Fig. S3†) and the fluorescence emission properties (Fig. S4†) of the free ligand **L**$_3$ and of the Ga**L**$_3$ complex (Fig. 4) were studied in non-deoxygenated water (pH 7.0) by UV-Vis and steady-state fluorescence spectroscopy (Table 2).

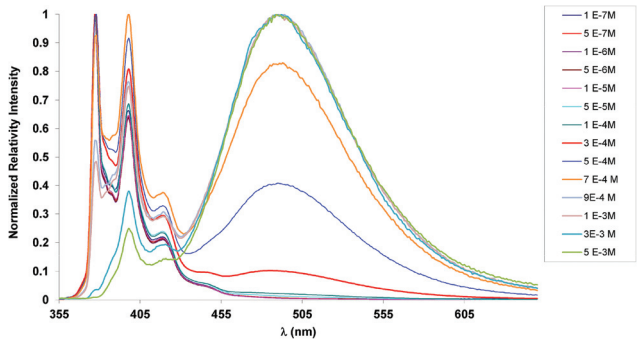

Fig. 4 Normalized fluorescence spectra for GaL_3 in non-deoxygenated water over the concentration range 5×10^{-7}–5×10^{-3} mol dm^{-3} (λ_{exc} = 345 nm).

Table 2 Quantum yields (Φ_F) for the ligand L_3 and GaL_3 complex (λ_{ex} 345 nm) in non-deoxygenated water

Φ_F [a,b]	
L_3	GaL_3
0.20	0.30

[a] Relative to anthracene in ethanol (Φ = 0.27). [b] Ligand and complex at 1.0×10^{-6} M concentration, non-deoxygenated solutions.

The absorption spectra of L_3 and GaL_3 (1×10^{-5} M, pH 7.0) exhibit bands in the wavelength range 300–350 nm characteristic of pyrene intraligand π–π* transitions (Fig. S3†).[47] The steady state fluorescence spectra of L_3 (Fig. S4†) and GaL_3 (Fig. 4) at low micromolar concentrations (1×10^{-6} M, λ_{ex} = 345 nm) display the typical vibronically structured band, attributed to the pyrene monomer (^{1}π–π* transitions).[37,48] The fluorescence quantum yields for L_3 and for the pyrene-centred emission in GaL_3 are of the same order of magnitude as those reported for other pyrene conjugates.[37,47,48] Complex formation with diamagnetic Ga^{3+} enhances slightly the fluorescence quantum yield of L_3. The concentration dependence of the steady state fluorescence properties of L_3 (Fig. S4†) and GaL_3 (Fig. 4) indicates that both, ligands and complex, undergo self-assembly, presumably into micelle-type structures, in aqueous solution.

Increasing the concentration of L_3 and GaL_3 triggers a gradual switch from the characteristic structured pyrene monomer spectrum to the broad featureless typical excimer (excited dimer) spectrum, indicating self-assembly in solution, presumably in the form of micelle-type structures.[37] Attempts to calculate the critical micelle concentration (cmc) for L_3 and GaL_3, by fitting the concentration dependence of the ratio of fluorescence emission intensities for the *excimer* (490 nm) and for the monomer (377 nm) (I_E/I_M) to a sigmoidal curve model, proved unsuccessful.[37,49,50] Nonetheless, the aggregation-sensitive nature of the fluorescence emission is clearly observable. Above the cmc, aggregates and monomers (at a concentration equal to the cmc value) are present in solution. Increasing the ligand or chelate concentration leads to an increase of the number of micelles, enhancing excimer emission.

In vitro stability and biodistribution studies

The kinetic stability of the $[^{67}Ga]L_2$ chelate towards *in vivo* transchelation was assessed by incubating the $^{67}Ga^{3+}$-labeled chelate with fresh human serum, followed by precipitation of the protein fraction and measurement of the activity in the pellet and in the soluble fraction (Fig. 5).

The percentage of total activity in the protein pellet reached immediately a value of 10% after incubating the complex with serum. This value remained constant over 1 hour incubation, revealing early association of the complex with blood proteins, presumably involving the lipophilic benzoyl moiety (Log $P_{calculated}(GaL_2)$ = 0.69, see ESI†). Radio-TLC analysis of the soluble fraction after 1 hour incubation revealed that the complex remains intact.

Biodistribution profiles were obtained for the $[^{67}Ga]L_3$ labelled complex at 1 and 24 hour post-injection in Wistar rats (Fig. 6, Table S1†).

At 1 hour post-injection the activity is manly located in the kidneys, liver and blood and to a lesser extent in the lungs and intestines. The high kidney uptake, compared to liver, indicates that the main elimination pathway is renal. The relatively high activity in the blood at 1 hour post injection suggests association of the complex with plasma proteins, probably

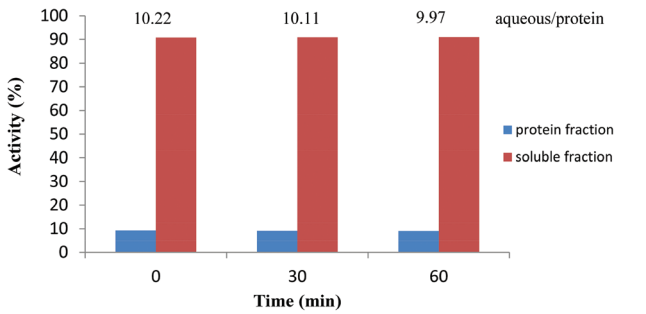

Fig. 5 Percentage of activity in the protein and in the soluble fraction at different incubation times of $[^{67}Ga]L_2$ with human serum.

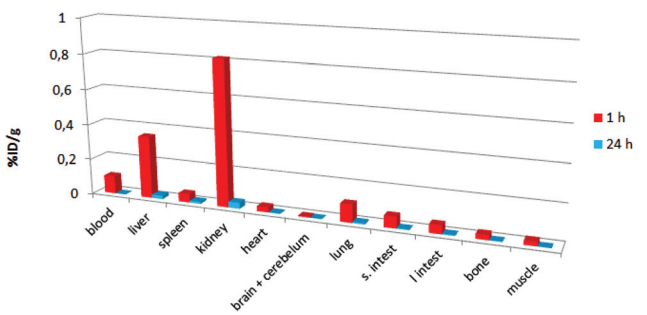

Fig. 6 Biodistribution profiles, presented as % injected activity per gram of organ or tissue, for the $[^{67}Ga]L_3$ complex at 1 and 24 hours post-injection. Results are the average of 4 animals.

albumin or lipoproteins, presumably through the lipophilic pyrene moiety (Log $P_{calculated.}$(Ga**L**$_3$) = 3.31, see ESI†).[37] The very low spleen and lung uptake suggests that in the blood the complex is not aggregated. A motivating factor for performing the biodistribution study was to ascertain potential brain uptake of Ga**L**$_3$. Biodistribution studies of the analogous [^{153}Sm][DO3A-*N*-(α-pyrenebutanamido)propionate] complex suggested a low, although not negligible, activity uptake at the brain-cerebellum at 1 hour pi.[37] The higher lipophilicity of Ga**L**$_3$ (overall neutral complex), compared to its DOTA analogue Sm[DO3A-*N*-(α-pyrenebutanamido)propionate] complex (overall charge −1), could conceivably result in higher brain uptake. The current study excludes brain uptake of [^{67}Ga]**L**$_3$. Most importantly, no significant activity remains in the liver and spleen and there is no activity deposition in the bones after 24 hours, indicating that complex demetallation is not occurring *in vivo*.

Conclusions

In this work we extend the synthetic pathways, reported previously for the DO3A-*N*-(α-amino)propionate family of chelators, to the triazacyclononane scaffold. A reversible pH-triggered switch from Ga^{3+} coordination to the carboxylate group of the substituted propionate arm (at pH values below 4.0) to amine coordination (at pH values above 6.0) was uncovered by ^{1}H and ^{71}Ga NMR studies of the Ga[NO2A-*N*-(α-amino)propionate] complex. The Ga^{3+} chelate of the benzoylamide conjugate displays pH-independent Ga^{3+} complexation to the carboxylate of the amide-substituted propionate arm in the pH range 3–11. Both complexes are stable in the physiological pH range. Moreover, the [^{67}Ga][NO2A-*N*-(α-benzoylamido)propionate] chelate is also stable in human serum. The pyrenebutyric acid conjugate, Ga[NO2A-*N*-(α-pyrenebutanamido)propionate] chelate, was designed as a potential bimodal PET/fluorescence imaging agent with aggregation-sensitive fluorescence properties.

The facile synthesis of conjugates of the NO2A-*N*-(α-amino)-propionic acid chelator, together with the serum stability of their Ga^{3+} chelates and fast renal elimination of the lipophilic pyrene conjugate, without any liver/spleen retention and activity deposition in the bones, warrants further evaluation of this novel class of chelators as potential tracers for PET. The reversible pH-triggered coordination switch demonstrated for the Ga[NO2A-*N*-(α-amino)propionate] complex can conceivably be translated into a method for pH measurement *in vivo* by ^{71}Ga NMR.

Experimental

Materials and methods

Chemicals were purchased from Sigma-Aldrich and used without further purification. Analytical grade solvents were used without further purification, unless otherwise specified. Reactions were monitored by TLC on a Kieselgel 60 F254 (Merck) on an aluminum support, with detection by examination under UV light (254 nm and 365 nm), by adsorption of iodine vapor and by spraying with ninhydrin. Flash chromatography was performed on a Kieselgel 60 (Merck, mesh 230–400). Ion exchange chromatography was performed on Dowex-1X2-OH$^-$ resin (Sigma Aldrich). The resin was purchased as the Cl$^-$ form and converted to the OH$^-$ form by the standard procedure. The relevant fractions from chromatography were pooled and concentrated under reduced pressure, T < 40 °C. ^{1}H and ^{13}C NMR spectra (assigned by 2D DQF-COSY and HMQC techniques) were run on a Varian Unity Plus 300 and a Bruker Avance-3 400 Plus NMR spectrometer, operating at 299.938 MHz and 75.428 MHz, and 400.13 MHz and 100.61 MHz, for ^{1}H and ^{13}C, respectively. ^{1}H 1D and 2D DQF-COSY and NOESY spectra were also run on a Varian VNMRS 600 at 599.72 MHz. Chemical shifts (δ) are given in ppm relative to the $CDCl_3$ solvent (^{1}H, δ 7.27; ^{13}C 77.36) as an internal standard. For ^{1}H and ^{13}C NMR spectra recorded in D_2O, chemical shifts (δ) are given in ppm, respectively, relative to TSP as an internal reference (^{1}H, δ 0.0) and *tert*-butanol as an external reference (^{13}C, CH_3 δ 30.29). ^{71}Ga NMR spectra were recorded at 122.026 MHz on a Bruker Avance-3 400 Plus spectrometer, using the signal of $[Ga(H_2O)_6]^{3+}$ present in a 0.1 M $Ga(NO_3)_3$ solution in D_2O, at 0 ppm as an external reference. pH measurements were performed on a pH meter Crison micro TT 2050 with an electrode Mettler Toledo InLab 422. For D_2O solutions, the isotopic correction pD = pH + 0.4 was done.[51] Mass spectrometry was performed at CACTI, Vigo, Spain.

Synthetic procedures

Preparation of monoalkylated nonanes 5, 6 and 7

*Synthesis of bis(*tert*-butoxycarbonyl)amino-methoxycarbonyl-ethyl-1,4,7-triaza cyclononane – monoalkylated nonane (5).* Boc_2-Δ-Ala-OMe (**2**) (158 mg, 0.51 mmol) was added in one portion to a suspension containing 1,4,7-triazacyclononane (98 mg, 0.76 mmol) and K_2CO_3 (279 mg, 2.0 mmol) in MeCN (20 mL). The suspension was vigorously stirred at room temperature for 2 hours. The suspended solid was removed by filtration and the solvent was evaporated under reduced pressure. The residue was purified by flash chromatography (100% CH_2Cl_2 → CH_2Cl_2–EtOH–NH_4OH–H_2O (50 : 50 : 1 : 1)) to afford compound **5** (120 mg, 55%). ^{1}H NMR (300 MHz, $CDCl_3$): δ = 1.51 (s, 18 H, Boc), 2.58–2.80 (m, 12 H, N(CH_2)$_2$N), 3.65 (dd, J = 14.1 and 8.4 H z, 1 H, A*B*X), 3.70 (dd, J = 14.1 and 4.5 Hz, 1 H, *A*BX), 3.71 (s, 3 H, C(O)OMe), 5.01 (dd, J = 8.4 and 4.5 Hz, 1 H, AB*X*).^{13}C NMR (75.4 MHz, $CDCl_3$): 28.02 (C(CH_3)$_3$), 46.45 (CH_2), 46.83 (CH_2), 52.16 (C(O)OCH_3), 53.16 (CH_2), 56.52 (CH_2), 56.67 (CH), 83.34 (C(CH_3)$_3$), 152.28 (C(O), carbamate), 170.73 (C(O), ester). HRMS (ESI): *m*/*z*: calcd for $C_{20}H_{39}N_4O_6$, $[M + H]^+$: 431.2864, found: 431.2859.

Synthesis of N-tert*-butoxycarbonylbenzamido-methoxycarbonyl-ethyl-1,4,7-triaza cyclononane – monoalkylated nonane (6).* (Benzyl)Boc-Δ-AlaOMe (**3**) (385 mg, 1.23 mmol) was added in one portion to a suspension containing 1,4,7-triazacyclo-

nonane (242 mg, 1.87 mmol) and K_2CO_3 (691 mg, 4.5 mmol) in MeCN (70 mL). The suspension was vigorously stirred at room temperature for 3 hours. The suspended solid was removed by filtration and the solvent was evaporated under reduced pressure. The residue was purified by flash chromatography (100% CH_2Cl_2 → CH_2Cl_2–EtOH–NH_4OH–H_2O (70 : 30 : 1 : 1)) to afford monoalkylated nonane **6** as a viscous light yellow oil (364 mg, 59%). ^{1}H NMR (300 MHz, $CDCl_3$): δ = 1.47 (s, 9 H, C(C*H*$_3$)$_3$), 2.50–2.90 (m, 12 H, N(C*H*$_2$)$_2$N), 3.01 (dd, *J* = 14.1 and 6.0 Hz, 1 H, A*B*X), 3.49 (dd, *J* = 14.4 and 5.1 Hz, 1 H, A*B*X), 3.76 (s, 3 H, C(O)OMe), 5.25 (t, *J* = 6.0 and 5.1 Hz, 1 H, AB*X*), 7.30–7.70 (5 H, m, Ar). ^{13}C NMR (75.4 MHz, $CDCl_3$): δ = 27.27 (C(*C*H$_3$)$_3$), 44.77 (CH$_2$), 45.83 (CH$_2$), 46.70 (CH$_2$), 51.27 (CH$_2$), 52.51 (C(O)O*C*H$_3$), 55.61 (N*C*H$_2$CH), 56.08 (*C*H), 83.88 (*C*(CH$_3$)$_3$), 127.87 (Ar), 127.96 (Ar), 131.27 (Ar), 137.02 (Ar), 152.72 (C(O), carbamate), 170.57 (C(O), amide), 172.62 (C(O), ester). HRMS (ESI): *m*/*z*: calcd for $C_{22}H_{35}N_4O_5$, $[M + H]^+$: 435.2602, found: 435.2601.

*Synthesis of methoxycarbonyl-(2-(*N-t-*butoxycarbonyl-4-pyrenebutanamido))-ethyl-4,7-bis-(ethoxycarbonylmethyl)-1,4,7-triazacyclononane – monoalkylated 7.* (Pyrenyl)Boc-Δ-AlaOMe (**4**) (1.01 g, 2.14 mmol) was added in one portion to a suspension containing 1,4,7-triazacyclononane (0.43 g, 3.33 mmol) and K_2CO_3 (1.76 g, 12.7 mmol) in MeCN (40 mL). The suspension was vigorously stirred at room temperature for 5 hours. The suspended solid was removed by filtration and the solvent was evaporated under reduced pressure. The residue was purified by flash chromatography (100% CH_2Cl_2 → CH_2Cl_2–EtOH–NH_4OH–H_2O (70 : 30 : 1 : 1)) to afford monoalkylated nonane **7** as a viscous light yellow oil (0.76 g, 59%). ^{1}H NMR (300 MHz, $CDCl_3$): δ = 1.42 (s, 9 H, C(C*H*$_3$)$_3$), 2.21 (m, 2 H, NHC(O)-CH$_2$*CH*$_2$), 2.64 (m, 8 H, 2 × N(*CH*$_2$)$_2$N), 2.90 (m, 1 H, A*B*X), 3.12 (m, 6 H, N(*CH*$_2$)$_2$N and NHC(O)*CH*$_2$), 3.38–3.50 (m, 3 H, NHC-(O)CH$_2$CH$_2$*CH*$_2$ and A*B*X), 3.43 (m, 2 H, N(*CH*$_2$)$_2$N), 3.70 (s, 3 H, C(O)OMe), 5.44 (t, *J* = 6.9 and 4.8 Hz, 1 H, AB*X*), 7.95–8.40 (9 H, m, Ar). ^{13}C NMR (75.4 MHz, $CDCl_3$): δ = 27.03 (CH$_2$), 27.83 (C(*C*H$_3$)$_3$), 32.83 (CH$_2$), 37.85 (CH$_2$), 45.71 (CH$_2$), 46.20 (CH$_2$), 46.45 (CH$_2$), 52.11 (CH$_2$), 52.20 (C(O)O*C*H$_3$), 54.24 (CH), 58.17 (N*C*H$_2$CH), 84.34 (*C*(CH$_3$)$_3$), 123.44 (Ar), 123.87 (Ar), 124.72 (Ar), 125.02 (Ar), 125.76 (Ar), 126.58 (Ar), 127.28 (Ar), 127.47 (Ar), 128.66 (Ar), 129.85 (Ar), 130.82 (Ar), 130.92 (Ar), 131.33 (Ar), 151.86 (C(O), carbamate), 170.75 (C(O), ester). HRMS (ESI): *m*/*z*: calcd for $C_{35}H_{45}N_4O_5$, $[M + H]^+$, 601.3390, found: 601.3407.

Synthesis of *tris*-alkylated nonanes 8, 9 and 10

*Synthesis of bis(*tert-*butoxycarbonyl)amino-methoxycarbonyl-ethyl-4,7-bis-(*tert-*butoxycarbonyl methyl)-1,4,7-triazacyclononane – tris-alkylated nonane **8**.* *tert*-Butyl bromoacetate (85 μL, 0.57 mmol) was added in one aliquot to a suspension containing monoalkylated compound **5** (100 mg, 0.23 mmol) and K_2CO_3 (125 mg, 0.90 mmol) in MeCN (20 mL). The suspension was vigorously stirred at room temperature for 3 hours. The suspended solid was removed by filtration and the solvent was evaporated under reduced pressure. The residue was purified by flash chromatography (100% CH_2Cl_2 → CH_2Cl_2–EtOH (50 : 50)) to afford tris-alkylated compound **8** (69 mg, 45%). ^{1}H NMR (300 MHz, $CDCl_3$): δ = 1.44 (s, 18 H, C(*CH*$_3$)$_3$, Boc), 1.65 (s, 18 H, C(C*H*$_3$)$_3$, ester), 2.75–3.78 (m(br) 12 H, N(C*H*$_2$)$_2$N), 3.03 (t, *J* = 4.2 Hz, 1 H, A*B*X), 3.20 (t, *J* = 4.2 Hz, 1 H, *A*BX), 3.73 (s, 4 H, N*CH*$_2$C(O)), 3.78 (s, 3 H, C(O)O*Me*), 5.01 (t, *J* = 4.2 Hz 1 H, AB*X*).^{13}C NMR (75.4 MHz, $CDCl_3$): 28.02 (C(*C*H$_3$)$_3$, Boc and ^{t}Bu ester), 44.53 (3 C, NCH*C*H$_2$, CH$_2$), 50.80 (2 C, CH$_2$), 53.16 (2 C, CH$_2$), 52.33 (3 C, OCH$_3$, 2 × CH$_2$), 56.52 (CH), 81.00 (2 C, *C*(CH$_3$)$_3$), 83.50 (2 C, *C*(CH$_3$)$_3$), 150.59 (1 C, C(O)), 151.98 (1 C, C(O), carbamate), 163.95 (1 C, *C*(O)OCH$_3$), 170.98 (2 C, C(O)). HRMS (ESI): *m*/*z*: calcd for $C_{32}H_{59}N_4O_{10}$, $[M + H]^+$, 659.4226, found: 659.4218.

*Synthesis of benzamido-methoxycarbonylethyl-4,7-bis-(ethoxycarbonylmethyl)-1,4,7-triaza cyclononane – tris-alkylated nonane **9**.* A solution of monoalkylated compound **6** (340 mg, 0.78 mmol) in trifluoroacetic acid in dichloromethane (60%, 25 mL) was stirred overnight at room temperature. The solvent was evaporated at reduced pressure. The residue was re-dissolved in dichloromethane and the solvent was evaporated. This procedure was repeated several times to give a light yellow thick oil. ^{1}H NMR spectroscopy ($CDCl_3$) revealed the disappearance of the signals assigned to the Boc group in the precursor compound. The oil (0.78 mmol, assuming quantitative deprotection) was dissolved in MeCN (30 mL), K_2CO_3 (1.0 g, 7.8 mmol) was added and the suspension was vigorously stirred at room temperature for 15 minutes. Ethyl bromoacetate (0.21 mL, 1.88 mmol) was added and the suspension was further stirred at room temperature for 2.5 hours. The suspended solid was removed by filtration, the solvent was evaporated under reduced pressure and the residue was purified by flash chromatography (100% CH_2Cl_2 → CH_2Cl_2–EtOH (7 : 3)) to afford compound **9** (355 mg, 37%) as a white foam. ^{1}H NMR (300 MHz, $CDCl_3$): δ = 1.22 (m, 6 H, C(O)OCH$_2$*CH*$_3$), 2.2–3.60 (broad multiplet, 18 H, N(*CH*$_2$)$_2$N, N*CH*$_2$C(O) and N*CH*$_2$CH), 3.71 (s, 3 H, C(O)O*CH*$_3$), 4.11 (t, *J* = 7.5 Hz, C(O)O*CH*$_2$CH$_3$), 5.14 (m (br), 1 H, NCH$_2$*CH*), 7.44–8.03 (5H, m, Ar). ^{13}C NMR (75.4 MHz, $CDCl_3$): selected signals: 13.95 (C(O)OCH$_2$*C*H$_3$), 48.74 (CH), 49.04 (CH$_2$), 50.38 (CH$_2$), 51.48 (CH$_2$), 52.59 (CH$_2$), 52.95 (C(O)O*C*H$_3$), 53.62 (N*C*H$_2$CH), 53.62 (CH$_2$), 54.86 (CH$_2$), 54.96 (CH$_2$), 55.19 (CH$_2$), 55.37 (CH$_2$), 55.75 (CH$_2$), 56.18 (CH$_2$), 60.62 (CH$_2$), 60.94, 61.13, 61.21 (C(O)O*C*H$_2$), 127.83 (Ar), 128.12 (Ar), 128.41 (Ar), 131.53 (Ar), 131.84 (Ar), 132.62 (Ar), 167.79 (C(O), amide), 170.29 (2 × *C*(O), ethyl ester), 170.52 (*C*(O), methyl ester), 170.91 (*C*(O), ethyl ester). HRMS (ESI): *m*/*z*: calcd for $C_{25}H_{39}N_4O_7$, $[M + H]^+$, 507.2813, found: 507.2807.

*Synthesis of 1-(4-pyrenebutanamido)-carboxyethyl-4,7-bis-(ethoxycarbonylmethyl)-1,4,7-triaza cyclononane – tris-alkylated nonane **10**.* A solution of monoalkylated nonane **7** (0.69 g, 1.16 mmol) in trifluoroacetic acid in dichloromethane (60%, 25 mL) was stirred overnight at room temperature. The solvent was evaporated at reduced pressure. The residue was re-dissolved in dichloromethane and the solvent was evaporated. This procedure was repeated several times to give a light yellow thick oil. ^{1}H NMR spectroscopy ($CDCl_3$) revealed the disappearance of the signals assigned to the Boc group in precursor **7**. The oil (1.16 mmol, assuming quantitative deprotection)

was dissolved in MeCN (30 mL), K_2CO_3 (1.6 g, 11.5 mmol) was added and the suspension was vigorously stirred at room temperature for 15 minutes. To this suspension was added ethyl bromoacetate (0.31 mL, 2.77 mmol). The suspension was vigorously stirred at room temperature overnight. The suspended solid was removed by filtration, the solvent was evaporated under reduce pressure and the residue was purified by flash chromatography (100% CH_2Cl_2 → CH_2Cl_2–EtOH (1 : 1)) to afford compound **10** (0.425 g, 55%) as a white foam. ^{1}H NMR (300 MHz, $CDCl_3$): δ = 1.26 (m, 6 H, 2 × C(O)OCH$_2$*CH*$_3$), 2.24 (m, 2 H, NHC(O)CH$_2$*CH*$_2$), 2.44 (m, 2 H, NHC(O)*CH*$_2$), 2.60–2.90 (m, 4 H, N*CH*$_2$C(O)), 2.50–3.40 (m, 16 H, N(*CH*$_2$)$_2$N, N*CH*$_2$C(O), N*CH*$_2$CH), 3.37 (m, 2 H, NHC(O)(CH$_2$)$_2$*CH*$_2$), 3.73 (s, 3 H, C(O)OMe), 3.92 (m, 4 H), 4.10 (m, 6 H, C(O)O*CH*$_2$), 4.81(d(br), 1 H, NCH$_2$*CH*), 7.80–8.40 (9 H, m, Ar). ^{13}C NMR (75.4 MHz, $CDCl_3$): selected signals: 14.05 and 14.13 (C(O)OCH$_2$*C*H$_3$), 27.23 (NHC(O)CH$_2$*C*H$_2$), 32.67 (NHC(O)(CH$_2$)$_2$-*C*H$_2$), 35.39 (NHC(O)*C*H$_2$), 43.50 (CH$_2$), 43.76 (CH$_2$), 43.98 (CH$_2$), 48.06 (CH$_2$), 51.22 (CH$_2$), 51.72(CH$_2$), 51.86 (C(O)O*C*H$_3$), 52.51 (CH), 52.60 (CH$_2$), 55.40 (CH$_2$), 55.64 (CH$_2$), 60.82, 60.98 (C(O)O*C*H$_2$), 123.63 (Ar), 124.62 (Ar), 124.75 (Ar), 124.85 (Ar), 125.76 (Ar), 126.51 (Ar), 127.18 (Ar), 127.41 (Ar), 127.46 (Ar), 128.67 (Ar), 129.72 (Ar), 130.87 (Ar), 131.32 (2 × Ar), 136.43 (C), 136.53 (Ar), 171.36 (*C*(O), ethyl ester), 171.39 (*C*(O), ethyl ester), 171.54 (*C*(O), methyl ester), 173.64 (*C*(O), amide).

Synthesis of fully deprotected ligands L_1, L_2 and L_3

*Synthesis of aminocarboxyethyl-4,7-bis-(carboxymethyl)-1,4,7-triazacyclononane – fully deprotected NO2A-*N*-(α-amino)propionic acid ligand (**L$_1$**).* A solution of prochelator **8** (50 mg, 0.076 mmol) in a mixture of hydrochloric acid 6 M–ethanol (12 mL; 2/1 (v/v)) was stirred at room temperature for 2 hours. The solvent was evaporated under reduced pressure and the residue was re-dissolved in a mixture of water–ethanol (10 mL; 1/1 (v/v)). The solution was adjusted to pH ~ 10 with Dowex-1X2100-OH$^-$ resin (10 mL, wet resin) and the suspension was stirred for 1 hour at room temperature. The resin was transferred into a column, washed with water and further eluted with hydrochloric acid 0.1 M. The relevant fractions, identified by TLC (ethanol–water 1/1, revelation with iodine vapor) were pooled together and evaporated at reduced pressure to afford ligand **L$_1$** in the hydrochloride form as an off-white solid (25 mg, quantitative yield).^{1}H NMR (300 MHz, D_2O): δ = 2.73–3.67 (m, 16 H, N(CH$_2$)$_2$N and N*CH*$_2$CO$_2$H), 3.06 (d, *J* = 3.9 Hz and x Hz, 1 H, A*B*X), 3.31 (dd, *J* = 12.3 and 3.9 Hz, 1 H, *A*BX), 5.01 (dd, *J* = 10.5 and 3.9 Hz, 1 H, AB*X*). ^{13}C NMR (75.4 MHz, D_2O): 48.71 (CH$_2$), 49.04 (CH$_2$), 49.50 (CH$_2$), 50.93 (CH$_2$), 51.68 (CH$_2$), 53.35 (CH), 57.31 (CH$_2$), 57.93 (CH$_2$), 58.46 (CH$_2$), 173.31 (CO$_2$H), 174.99 (CO$_2$H), 176.42 (CO$_2$H). HRMS (ESI) *m*/*z*: calcd for $C_{13}H_{25}N_4O_6$ $[M + H]^+$: 333.1769, found: 333.1769.

*Synthesis of benzamido-carboxyethyl-4,7-bis-(carboxymethyl)-1,4,7-triazacyclononane – fully deprotected NO2A-*N*-(α-benzoyl-amido)propionic acid ligand (**L$_2$**).* Prochelator (**9**) (323 mg, 0.89 mmol) was dissolved in a mixture of ethanol–water (20 mL, 1/1 (v/v)). The solution was adjusted to pH ~ 10 by adding small portions of Dowex-1X2-100-OH$^-$ resin. The suspension was stirred gently at room temperature for 2 hours. The wet resin was transferred into a chromatography column, washed with water (~50 mL) and eluted with hydrochloric acid 0.1 M. The relevant fractions, identified by TLC (ethanol–water 1/1, revelation with iodine vapor), were pooled, concentrated at room temperature and further dried under vacuum to afford ligand **L$_2$**, in the hydrochloride form, as a light yellow solid (180 mg, 71%). ^{1}H NMR (300 MHz, D_2O): δ = 2.9–3.6 (broad, overlapped signals with an integration corresponding to 14 H, N(*CH*$_2$)$_2$N and NC*CH*$_2$CH), 3.81 (broad, overlapped signals with an integration corresponding to 4 H, NC*H*$_2$CO$_2$H), 4.80 (m (broad), 1 H, C*H*), 7.53–7.88 (5 H, m, Ar). ^{13}C NMR (75.4 MHz, D_2O): selected signals: 43.02 (CH$_2$), 48.11 (CH$_2$), 48.93 (CH$_2$), 49.03 (CH$_2$), 49.78 (CH$_2$), 51.39 (CH$_2$), 51.71 (CH), 51.91 (CH$_2$), 54.53 (CH$_2$), 56.08 (CH$_2$), 56.77 (CH$_2$), 127.46 (Ar), 129.04 (Ar), 132.60 (Ar), 133.32 (Ar), 170.20 (CO$_2$H), 177.17 (C(O), amide). HRMS (ESI): *m*/*z*: calcd for $C_{20}H_{29}N_4O_7$, $[M + H]^+$, 437.2031, found: 437.2027.

*Synthesis of 1-(4-pyrenebutanamido)-carboxyethyl-4,7-bis-(carboxymethyl)-1,4,7-triazacyclononane – fully deprotected NO2A-*N*-(α-pyrenebutanamido)propionic acid ligand (**L$_3$**).* Prochelator (**10**) (0.360 g, 0.53 mmol) was dissolved in a mixture of ethanol–water (1/1 v/v, 20 mL). The solution was adjusted to pH ~ 10 by adding small portions of Dowex-1X2-100-OH$^-$ resin. The suspension was kept under stirring at room temperature for 2 hours. The wet resin was transferred into a chromatography column, washed with water (~50 mL) and eluted with 0.1 M hydrochloric acid, followed by a mixture of hydrochloric acid 0.2 M–ethanol (1/1 v/v). The relevant fractions, identified by TLC (ethanol–water, 1/1 v/v, revelation with iodine vapor and visualization under UV light λ_{365} nm), were pooled, concentrated at room temperature and further dried under vacuum to afford deprotected chelator **L$_3$** in the hydrochloride form, as a light yellow solid (0.149 g, 46%). ^{1}H NMR (400 MHz, D_2O/CD_3OD): δ = 1.9–3.3 (broad, overlapped signals with an integration corresponding to 24 H, NHC(O)*CH*$_2$*CH*$_2$*CH*$_2$, N*CH*$_2$CO$_2$H, N*CH*$_2$CH and N(*CH*$_2$)$_2$N), 4.49 (m (br), 1 H, *CH*), 7.80–8.40 (9 H, m, Ar). ^{13}C NMR (75.4 MHz, D_2O/CD_3OD): selected signals: 28.22 (NHC(O)CH$_2$*CH*$_2$), 33.25 ((NHC(O)-(CH$_2$)$_2$*CH*$_2$), 36.23 ((NHC(O)*CH*$_2$), 48.92 (CH), 50.49 (CH$_2$), 54.95 (CH$_2$), 122.75 (Ar), 123.97 (Ar), 124.03 (CH-Ar), 124.58 (2 × (CH-Ar)), 125.71 (CH-Ar), 126.19 (CH-Ar), 126.93 (C-Ar), 126.99 (CH-Ar), 127.28 (CH-Ar), 127.92 (CH-Ar), 129.24 (C-Ar), 130.20 (C-Ar), 130.70 (C-Ar), 135.44 (C-Ar), 171.98 (CO$_2$H), 172.19 (2 × CO$_2$H), 175.41 (NH*C*(O)). HRMS (ESI): *m*/*z*: calcd for $C_{33}H_{38}N_4NaO_7$, $[M + Na]^+$, 625.2638, found: 625.2621.

Preparation of Ga^{3+} chelates for ^{1}H and ^{71}Ga NMR. To an aqueous solution of the ligand (pH = 3.0) was added dropwise an aqueous solution of $GaCl_3$ in a 1 : 1 mole ratio. The pH was kept below 3.8 by the addition of aqueous NaOH. The solution was stirred at room temperature overnight and the solvent was removed at reduced pressure. Solutions for NMR measurements (20 mM, D_2O) were obtained by dissolution of the solid complexes in D_2O (0.75 mL). ^{1}H and ^{71}Ga NMR spectra of the complexes were obtained at 298 K on a Bruker Avance-3 400 Plus spectrometer, operating at 400.02 and 121.98 MHz,

respectively. The proton NMR spectra of the complexes were assigned by 2D COSY and NOESY techniques using a Varian VNMRS 600 NMR spectrometer. The ^{1}H and ^{71}Ga NMR pH study of the complexes was performed by adding small portions of NaOD or DCl to the complex solutions to obtain the desired pH.

Fluorescence measurements

The absorption and the fluorescence emission spectra of the free ligand $\mathbf{L_3}$ and the Ga$\mathbf{L_3}$ complex were recorded, respectively, with a Jasco V-630 UV-Vis spectrophotometer and a HORIBA Jobin Yvon Fluoromax-4 spectrofluorimeter, equipped with a monochromator in both excitation and emission and a temperature controlled cuvette holder. Fluorescence spectra were corrected for the instrumental response of the system. The fluorescence quantum yields (Φ_F) were determined using the standard method.[52,53] Anthracene in ethanol (Φ_r = 0.27)[54] was used as a reference.

Radiochemistry

$^{67}Ga^{3+}$ complexes for *in vivo* and *in vitro* experiments were prepared by adding 1 mCi of [^{67}Ga]citrate (produced at IBA Molecular, Louvain-la-Neuve) to a solution of 1 mg of the chelator in HEPES buffer (400 μL, 0.4 M, pH 4) and heated at 80 °C for *ca*. 1 hour. The radiochemical purity of the final products was determined by TLC. The percentage of the bound metal was above 95% in all cases.

Calculation of log *P*

The lipophilicity of Ga$\mathbf{L_2}$ and Ga$\mathbf{L_3}$ complexes was assessed by computing their log *P* values using the ALOGPS software (free software available at http://www.vclab.org/lab/alogps).[55]

Stability in blood serum

For the blood serum stability studies, 5 μCi of a standard solution of [^{67}Ga]$\mathbf{L_2}$ were added to 5 mL of fresh human serum, previously equilibrated in 5% CO_2 (95% air) environment at 37 °C. The mixture was kept in the same environment, and aliquots of 100 μL (in triplicate) were taken at appropriate periods of time (0 min, 30 min, and 1 hour). The aliquots were treated with 200 μL of ethanol, cooled (4 °C), and centrifuged for 15 min at 4000 rpm, at 4 °C, in order to precipitate the serum proteins. A 100 μL aliquot of supernatant was collected for activity counting in a γ well-counter. The sediment was washed twice with 1 mL of EtOH and its activity was counted. The activity of the supernatant was compared to that of the sediment in order to determine the percentage of the chelate associated with the proteins. The activity of the supernatant at 1 hour was evaluated by TLC in order to check whether the chelate remained intact.

Biodistribution studies

All animal studies were performed by authorized researchers in strict adherence to the Portuguese laws for animal protection.

Groups of four animals (Wistar male rats weighting *ca*. 200 g) were anaesthetized with ketamine (50.0 mg mL^{-1})–chloropromazine (2.5%) (10 : 3), injected in the tail vein with *ca*. 100 μCi of [^{67}Ga]$\mathbf{L_3}$ and sacrificed 1 and 24 hours later. The major organs were removed, weighed and counted in a γ well-counter. The biodistribution is stated as percentage of injected dose per gram of organ (%ID g^{-1}).

Acknowledgements

This work was financially supported by Fundação para a Ciência e Tecnologia, Portugal (PEst-C/QUI/UI0686/2013; FCOMP-01-0124-FEDER-037302; PTDC/QUI/70063/2006); grant SFRH/BD/63994/2009 to Miguel Ferreira and sabbatical grant SFRH/BSAB/1328/2013 to J. A. Martins; and Rede Nacional de RMN (REDE/1517/RMN/2005) for the acquisition of the Varian VNMRS 600 NMR spectrometer at the University of Coimbra and the Bruker Avance-3 400 Plus at the University of Minho in Braga. We also acknowledge the COST Action TD1004 "Theragnostics Imaging and Therapy".

References

1 Z. Li and P. S. Conti, *Adv. Drug Delivery Rev.*, 2010, **62**, 1031–1051.
2 I. Kayani and A. M. Groves, *Clin. Med.*, 2006, **6**, 240–244.
3 T. Ebenhan, M. Honer, S. M. Ametamey, P. A. Schubiger, M. Becquet, S. Ferretti, C. Cannet, M. Rausch and P. M. McSheehy, *Mol. Imaging Biol.*, 2009, **11**, 308–321.
4 F. Rösch and R. P. Baum, *Dalton Trans.*, 2011, **40**, 6104–6111.
5 M. Fani, J. P. André and H. R. Mäcke, *Contrast Media Mol. Imaging*, 2008, **3**, 53–63.
6 F. Rösch and P. J. Riss, *Curr. Top. Med. Chem.*, 2010, **10**, 1633–1668.
7 M. I. M. Prata, *Curr. Radiopharm.*, 2012, **5**, 142–149.
8 M. A. Green and M. J. Welsh, *Nucl. Med. Biol.*, 1989, **16**, 435–448.
9 S. Jurisson, D. Berning, W. Jia and D. Ma, *Chem. Rev.*, 1993, **93**, 1137–1156.
10 T. J. Wadas, E. H. Wong, G. R. Weisman and C. J. Anderson, *Chem. Rev.*, 2010, **110**, 2858–2902.
11 W. R. Harris and V. L. Pecoraro, *Biochemistry*, 1983, **22**, 292–299.
12 V. Kubicek, J. Havlicková, J. Kotek, G. Tircsó, P. Hermann, É. Tóth and I. Lukes, *Inorg. Chem.*, 2010, **49**, 10960–10969.
13 A. F. Martins, M. I. M. Prata, S. P. J. Rodrigues, C. F. G. C. Geraldes, P. J. Riss, A. Amor-Coarasa, C. Burchardt, C. Kroll and F. Rösch, *Contrast Media Mol. Imaging*, 2013, **8**, 265–273.
14 M. Bauwens, R. Chekol, H. Vanbilloen, G. Bormans and A. Verbruggen, *Nucl. Med. Commun.*, 2010, **31**, 753–758.
15 D. A. Moore, P. E. Fanwick and M. J. Welch, *Inorg. Chem.*, 1990, **29**, 672–676.

16 E. T. Clarke and A. E. Martell, *Inorg. Chim. Acta*, 1991, **181**, 273–280.
17 C. J. Broan, J. P. L. Cox, A. S. Craig, R. Kataky, D. Parker, A. Harrison, A. M. Randall and G. Ferguson, *J. Chem. Soc., Perkin Trans. 2*, 1991, 87–99.
18 J.-F. Morfin and É. Tóth, *Inorg. Chem.*, 2011, **50**, 10371–10378.
19 D. J. Hnatowich and P. Schiegel, *J. Nucl. Med.*, 1981, **22**, 623–626.
20 J. Schuhmacher, R. Matys, H. Hauser, W. Maierborst and S. Matzku, *Eur. J. Nucl. Med.*, 1986, **12**, 397–404.
21 R. Delgado, F. M. de Carmo and S. Quintino, *Talanta*, 1997, **45**, 451–462.
22 R. M. Smith and A. E. Martell, *Critical Stability Constants*, Plenum Press, New York, 1989.
23 A. Heppeler, S. Froidevaux, H. R. Mäcke, E. Jermann, M. Béhé, P. Powell and M. Hennig, *Chem.–Eur. J.*, 1999, **5**, 1974–1981.
24 A. Heppeler, J. P. André, I. Buschmann, X. Wang, J.-C. Reubi, M. Hennig, T. A. Kaden and H. R. Mäcke, *Chem.–Eur. J.*, 2008, **14**, 3026–3034.
25 I. Velikyan, H. Mäcke and B. Langstrom, *Bioconjugate Chem.*, 2008, **19**, 569–573.
26 A. de Sá, A. A. Matias, M. I. M. Prata, C. F. G. C. Geraldes, P. M. T. Ferreira and J. P. André, *Bioorg. Med. Chem. Lett.*, 2010, **20**, 7345–7348.
27 J. P. André, H. R. Mäcke, M. Zehnder, L. Macko and K. G. Akyel, *Chem. Commun.*, 1998, 1301–1302.
28 K. P. Eisenwiener, M. I. M. Prata, I. Buschmann, H. W. Zhang, A. C. Santos, S. Wenger, J. C. Reubi and H. R. Mäcke, *Bioconjugate Chem.*, 2002, **13**, 530–541.
29 J. Notni, P. Hermann, J. Havlíčková, J. Kotek, V. Kubíček, J. Plutnar, N. Loktionova, P. J. Riss, F. Rösch and I. Lukes, *Chem.–Eur. J.*, 2010, **16**, 7174–7185.
30 J. Šimeček, M. Schulz, J. Notni, J. Plutnar, V. Kubíček, J. Havlíčková and P. Hermann, *Inorg. Chem.*, 2012, **51**, 577–590.
31 J. Šimeček, J. Notni, V. Kubiček and P. Hermann, *Nucl. Med. Biol.*, 2010, **37**, 679.
32 A. N. Singh, W. Liu, G. Hao, A. Kumar, A. O. Z O. K. Gupta, J.-T. Hsieh and X. Sun, *Bioconjugate Chem.*, 2011, **22**, 1650–1662.
33 M. Studer and C. F. Meares, *Bioconjugate Chem.*, 1992, **3**, 337–341.
34 M. F. Ferreira, A. F. Martins, J. A. Martins, P. M. Ferreira, É. Tóth and C. F. G. C. Geraldes, *Chem. Commun.*, 2009, 6475–6477.
35 M. F. Ferreira, B. Mousavi, P. M. Ferreira, C. I. O. Martins, L. Helm, J. A. Martins and C. F. G. C. Geraldes, *Dalton Trans.*, 2012, **41**, 5472–5475.
36 M. F. Ferreira, A. F. Martins, C. I. O. Martins, P. M. Ferreira, É. Tóth, T. B. Rodrigues, D. Calle, S. Cerdan, P. Lopez-Larrubia, J. A. Martins and C. F. G. C. Geraldes, *Contrast Media Mol. Imaging*, 2013, **8**, 40–49.
37 M. F. Ferreira, G. Pereira, A. F. Martins, C. I. O. Martins, M. I. M. Prata, S. Petoud, E. Toth, P. M. T. Ferreira, J. A. Martins and C. F. G. C. Geraldes, *Dalton Trans.*, 2014, **43**, 3162–3173.
38 J. W. Akitt, in *Multinuclear NMR*, ed. J. Mason, Plenum Press, New York, 1987, ch. 9, pp. 259–288.
39 L. Ronconi and P. J. Sadler, *Coord. Chem. Rev.*, 2008, **252**, 2239–2277.
40 (*a*) J. P. André and H. R. Mäcke, *J. Inorg. Biochem.*, 2003, **97**, 315–323; (*b*) J. P. André, NMR Spectroscopy of Gallium in Biology, in *Encyclopedia of Metalloproteins*, ed. R. H. Kretsinger, V. N. Uversky and E. A. Permyakov, Springer, 2013.
41 A. S. Craig, D. Parker, H. Adams and N. A. Bailey, *J. Chem. Soc., Chem. Commun.*, 1989, 1793–1794.
42 D. Shetty, S. Y. Choi, J. M. Jeong, L. Hoigebazar, Y.-S. Lee, D. S. Lee, J.-K. Chung, M. C. Lee and Y. K. Chung, *Eur. J. Inorg. Chem.*, 2010, 5432–5438.
43 M. I. M. Prata, A. C. Santos, C. F. G. C. Geraldes and J. J. P. de Lima, *J. Inorg. Biochem.*, 2000, **79**, 359–363.
44 C. J. Broan, K. J. Jankowski, R. Kataky and D. Parker, *J. Chem. Soc., Chem. Commun.*, 1990, 1738–1739.
45 A. de Sá, M. I. M. Prata, C. F. G. C. Geraldes and J. P. André, *J. Inorg. Biochem.*, 2010, **104**, 1051–1062.
46 F. M. Winnik, *Chem. Rev.*, 1993, **93**, 587–614.
47 S. J. A. Pope, *Polyhedron*, 2007, **26**, 4818–4824.
48 J. P. Holland, V. Fisher, J. A. Hickin and J. M. Peach, *Eur. J. Inorg. Chem.*, 2010, 48–58.
49 C. Wang, S. D. Wettig, M. Foldvari and R. E. Verrall, *Langmuir*, 2007, **23**, 8995–9001.
50 C. Keyes-Baig, J. Duhamel and S. Wettig, *Langmuir*, 2011, **27**, 3361–3371.
51 P. K. Glasoe and F. A. Long, *J. Phys. Chem.*, 1960, **64**, 188–189.
52 J. N. Demas and G. A. Crosby, *J. Phys. Chem.*, 1971, **75**, 991–1024.
53 S. Fery-Forgues and D. Lavabre, *J. Chem. Educ.*, 1999, **76**, 1260–1264.
54 J. V. Morris, M. A. Mahaney and J. R. Huber, *J. Phys. Chem.*, 1976, **80**, 969–974.
55 I. V. Tetko, J. Gasteiger, R. Todeschini, A. Mauri, D. Livingstone, P. Ertl, V. A. Palyulin, E. V. Radchenko, N. S. Zefirov, A. S. Makarenko, V. Y. Tanchuk and V. V. Prokopenko, *J. Comput. Aided Mol. Des.*, 2005, **19**, 453–463.